Air Efficient Soft Wearable Robot for High-Torque Elbow Flexion Assistance

Harrison Young*,¹, Lucas Gerez*,¹, Tazzy Cole¹, Bianca Inirio¹, Tommaso Proietti¹, Bettie Closs¹, Sabrina Paganoni², and Conor Walsh^{1†}

Abstract—Recent developments in soft wearable robots have shown promise for assistive and rehabilitative use-cases. For inflatable approaches, a major challenge in developing portable systems is finding a balance between portability, performance, and usability. In this paper, we present a textile-based robotic sleeve that can provide functional elbow flexion assistance and is compatible with a portable actuation unit (PAU). Flexion is driven by a curved textile actuator with internal pneumatic supports (IPS). We show that the addition of IPS improves torque generation and increases battery-powered actuations by 60%. We demonstrate that the device can provide enough torque throughout the ROM of the elbow joint for daily life assistance. Specifically, the device generates 13.5 Nm of torque at 90°. Experimental testing in five healthy individuals and two individuals with Amyotrophic Lateral Sclerosis (ALS) demonstrates its impact on wearer muscle activity and kinematics. The results with healthy subjects show that the device was able to reduce the bicep muscle activity by an average of 49.1±13.3% during static and dynamic exercises, 43.6±11.1% during simulated ADLs, and provided an assisted ROM of 134°±13°. Both ALS participants reported a reduced rate of perceived exertion during both static and dynamic tasks while wearing the device and had an average ROM of 115°±8°. Future work will explore other applications of the IPS and extend the approach to assisting multiple joints.

I. Introduction

Elbow flexion is vital to the completion of self-care activities of daily living (ADLs). Many conditions such as spinal cord injury or neuromuscular diseases can cause severe elbow flexion impairment [1], [2]. Wearable robots are being investigated to help people who need active elbow flexion assistance. Robotic flexion assistance is difficult because the elbow joint requires a combination of both high torque and large range of motion (ROM) to complete important ADLs. [3], [4]. Design of wearable robots for flexion assistance is an area of active research and three types of robots are most common. Rigid exoskeletons generate a pure moment around the joint through mechanical linkages [5]. They are strong but rely on precise joint alignment and add greater mass to a limb. Tendon-driven exosuits pull a cable on either side of the joint. They generate high forces and are controllable

Research reported in this publication was supported by the National Science Foundation under awards EFRI 1830896 and DGE 1745303, the Office of Naval Research (ONR) award N00014-17-1-2121, and Harvard School of Engineering and Applied Sciences.

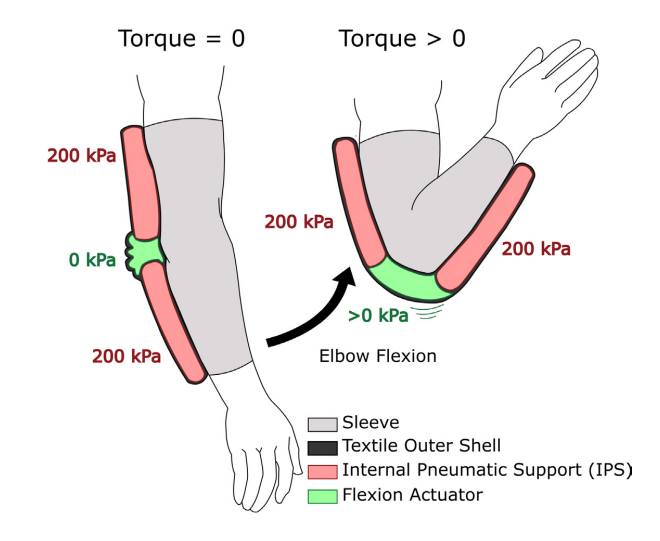


Fig. 1. Principle of operation of the proposed supported elbow flexion robot. The robot was designed to increase portability while maintaining performance and comfort. The actuator is composed of a flexion bladder (green) contained by two internal pneumatic supports (red).

but can be prone to slipping as forces react mostly in shear [6], [7]. Pneumatic soft robots are inflatable, often textile or elastomeric, structures that push on the joint. Textile-based wearable soft robots are lightweight, high torque, and can be integrated into clothing, offering the potential for a safe and comfortable solution for daily life assistance [8].

A variety of prototypes have been successfully implemented to help healthy and impaired populations in: opening and closing the hand [9], elevating the shoulder [10], flexing and extending the elbow [11]–[13], flexing and extending the knee [14]–[16] and supinating and pronating the wrist. [17].

For years textile-based wearable soft robots were limited to tethered systems. However, recently portable actuation units (PAU) capable of driving these robots have started to mature [8], [14], [18], [19]. Even with PAUs, actuator air consumption is a significant factor limiting portability. Researchers have been able to reduce air requirements by optimizing the dimensions of soft actuators or by constructing inflatable-rigid composite actuators that use inflatable actuators to generate torque and rigid structures to transmit it to the body [12], [19].

In this study, we propose a portable soft robotic sleeve that can provide assistance with elbow flexion (Fig. 1). We demonstrate the robot can provide enough torque throughout

Equal contribution.

John A. Paulson School of Engineering and Applied Sciences, Harvard University, Cambridge, MA 02138, USA.

² Department of Physical Medicine and Rehabilitation, Harvard Medical School, Spaulding Rehabilitation Hospital, Boston, MA 02129, USA.

[†] Corresponding author walsh@seas.harvard.edu

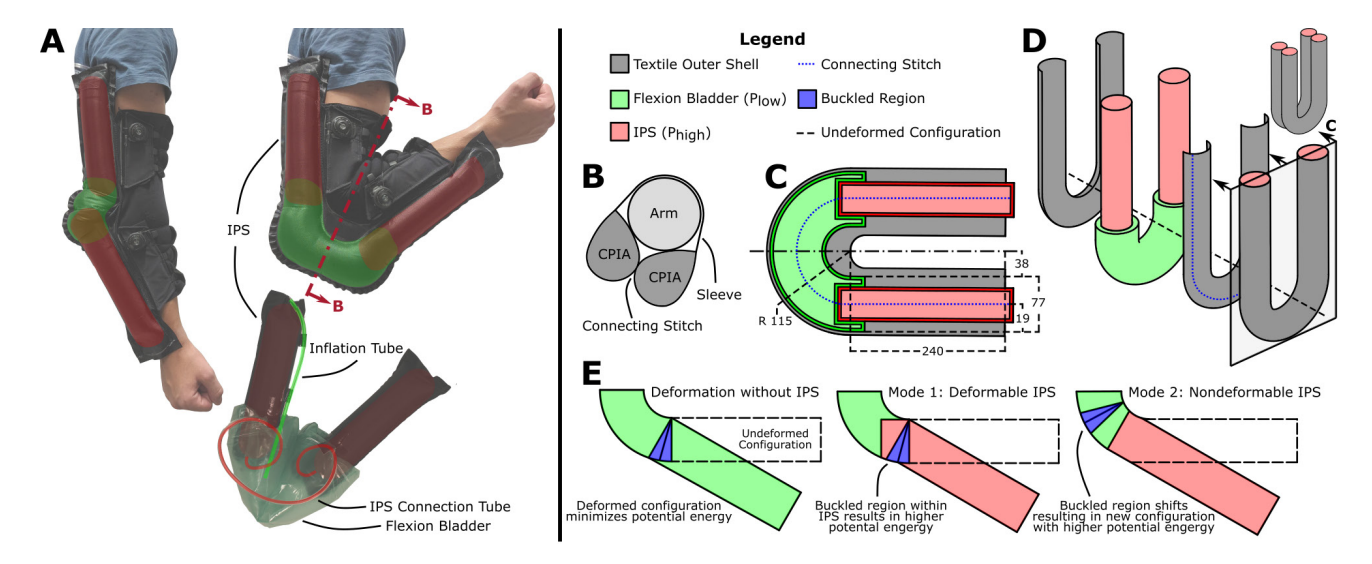


Fig. 2. A) Top: Elbow flexion robot during the flexion motion. The inflatable structural supports and the inflatable active region are highlighted in red and green, respectively. Bottom: Assembly of flexion bladder and IPS. B) Cross-section view showing the tilted orientation of the CPIAs on the arm. C) Exploded view of supported flexion actuator. D) Cross section of supported flexion actuator showing important dimensions (units in mm). E) Magnitude of assistance toque depends energy stored during actuator deformation. IPS increases energy stored by the actuator by supporting buckled the region of the CPIA. In mode 1, the actuator reaches its normal deformed configuration with the pressure in the buckled region at P_{high} . In mode 2, the IPS are non-deformable so the location of the buckled region must shift and the actuator is forced into a new deformed configuration.

the ROM of the elbow joint for the execution of ADLs. Internal pneumatic supports (IPS) simultaneously increase torque output while reducing air consumption of the robot, allowing for more actuation cycles when driven by a PAU. Experimental testing in five healthy individuals and two individuals with ALS demonstrates its impact on wearer muscle activity and kinematics.

II. ELBOW DEVICE DESIGN

A. Design Considerations

Wearable assistive robots require a balance between portability, performance, and usability. The performance specifications of our robot were determined based on the torque and ROM required to provide full assistance for most ADLs. The robot should provide at least 6 Nm of torque throughout most of its ROM [6] and be minimally restrictive as many important ADLs (eating, drinking, washing) require near maximal elbow flexion [3]. The torque and ROM of the robot are heavily influenced by its cross-sectional area and internal pressure. To practically assist ADLs, the robot needs to be comfortable enough to be worn for several hours. However, the arm is completely surrounded by sensitive soft tissue and, as a result, soft robots are often limited by user discomfort [11], [12]. One of the easiest ways to increase comfort is to lengthen the robot to distribute assistance force over a larger area on the arm [12]. There is a clear conflict between the strength and comfort required for a robot to be practically usable and the small volume required for portability.

B. Wearable Robot Overview

The robot is a sleeve with a U-shaped textile flexion actuator running along the posterior side of the arm centered around the elbow joint. The ends of each actuator are strengthened with IPS (Fig. 2.A). Both are made of inextensible woven fabric (500 denier nylon, Trident Textiles Corp, USA) enclosing an inflated TPU bladder (Stretchlon 200, Fiberglast, USA). The sleeve was designed to be one-size-fitsmost. The front of the sleeve is made from an extensible knit (Darlington Fabrics, USA) that allows it to loosely fit many different body sizes ranging between small and large. The precise fit necessary for torque transmission is achieved by tightening BOA mechanisms (BOA, Boa Technology, USA) on the arm and forearm. The textile construction makes the robot lightweight, only adding 300 grams to the arm.

C. Internal Pneumatic Supports (IPS)

The IPS are textile pressure vessels designed to reduce actuation volume by passively occupying the legs of the flexion actuator. This effectively decouples the robot's length from its air consumption allowing for both comfort and portability. Pressure vessels were used because they provide additional utility over truly passive foam or 3D printed structures. When inflated, the IPS expand inward and serve as a simple hands-free tightening mechanism for the sleeve. During use, the IPS are inflated once to tighten the sleeve during donning, remain pressurized while the sleeve is worn and are only deflated for doffing.

D. Flexion Actuator

The flexion actuator is an assembly of U-shaped curved pneumatic interference actuators (CPIA) joined side-by-side (Fig. 2.D), Each CPIA has a constant air channel width of 77 mm, an outer radius (R) of 115 mm and 240 mm long legs (Fig. 2.C). The two CPIAs are connected by sewing their two inward facing textile shells together via a connecting stitch located around 75% of the way up the air channel (19 mm from the seam line). The location of the connecting

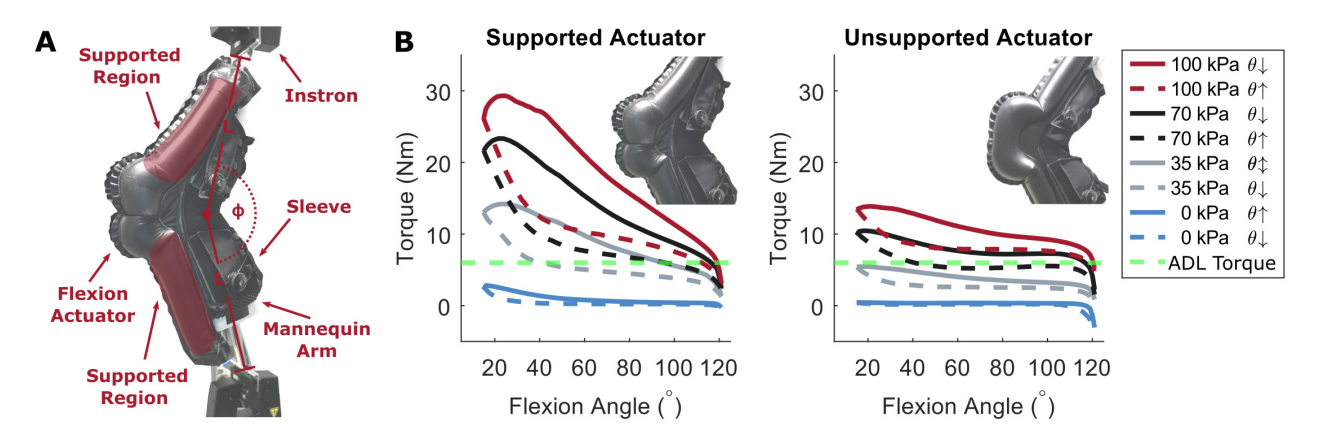


Fig. 3. A) Experimental setup. B) Results of mean torque test of the robot with supported flexion actuator (left) and unsupported flexion actuator (right) inflated to 0, 35 kPa, 70 kPa, and 100 kPa. The supported robot is capable of meeting or exceeding sufficient ADL torque through most of the ROM tested $(15^{\circ} - 118^{\circ})$ where $\theta = 180 - \phi$ and generates higher torque than its unsupported counterpart. Increase in torque is attributed to the IPS stiffening the distal regions and forcing the actuator into a new deformed configuration.

stitch causes the two CPIAs to tilt away from each other when inflated (Fig. 2.B). The CPIAs have a tear-drop shaped cross-section [20], tilting them widens the robot, making it more resistant to twisting and helping keep it centered on the arm. Flexion torque is produced by inflating a TPU bladder located in the curved part of the CPIA to $P_{flexion}$. An IPS is placed inside each leg such that one end protrudes into the flexion bladder (Fig. 2.A). The IPS are textile pressure vessels and will only be structurally stable if their internal pressure (P_{IPS}) exceeds the external pressure. This makes it essential that P_{IPS} always be greater than $P_{flexion}$. CPIAs generate torque when external loads cause the actuator to buckle, reducing its volume. The magnitude of the torque is modeled using the principle of virtual work [15], [16].

$$\tau(\theta, P) = -P \frac{\Delta V(\theta)}{\Delta \theta} \tag{1}$$

Where ΔV is the change in actuator volume due to buckling, P is the internal pressure of the buckled region, and θ is the angle of the deformation. All structures deform into a configuration that minimizes their potential energy. Similar CPIA deform symmetrically on the periphery of the actuator's curved region [16]. In our robot this weak region is supported by the high-pressure IPS (Fig. 2.E). We expect supporting the weak region will result in a stiffer actuator through two mechanisms: IPS may deform, meaning the pressure in the buckled region would increase from $P_{flexion}$ to P_{IPS} or the IPS may inhibit normal deformation and force the actuator into a new configuration with higher potential energy. Both are expected to result in higher torque values.

Benchtop testing was performed to characterize how IPS impact the torque of the robot. Previous work found the characterization of an isolated actuator fails to imitate on-body boundary conditions and may not accurately predict torque delivered to the wearer [21]. Therefore testing was performed using a full robot donned on a mannequin arm to approximate on-body boundary conditions. Two robots, with supported flexion actuators (with IPS) and unsupported flexion actuators (TPU bladder only and IPS removed),

were evaluated. Each trial consisted of cyclically loading the mannequin arm twice from 15° to 120° (with 0° corresponding to full elbow extension) at a constant vertical rate of 100 mm/min using a universal material tester (Instron 5566, Instron Corporation, USA) (Fig. 3.A). The robot was actuated with constant $P_{flexion}$ of 0, 35, 70, and 100 kPa. Each pressure trial was repeated 3 times, and the pressure order was randomized. Pressure was controlled using a precision pressure regulator (SMC IR2010-N02B, SMC Corporation, Japan). During all trials, IPS were inflated to 200 kPa using a separate regulator (Wilkerson R21-02-000, Wilkerson Corporation, USA). Results were zeroed from a baseline measurement obtained by driving the bare mannequin arm.

Fig. 3.B shows the torque output results of the benchtop experiments. The supported robot is able to maintain the target assistance torque of 6 Nm throughout most of the tested ROM (15°-118°). The torque suddenly drops off above 118° due to fabric bunching in the hinge of the mannequin arm. At 90° the robot is capable of producing 13.5 Nm of assistive torque, equivalent to offsetting 4 kg in the hand assuming a forearm + hand length of 0.34 m. The torque output curves are hysteretic. Hysteresis is a known limitation of soft inflatable textile actuators.

The supported robot generated 41% more torque than the unsupported robot at 90° (9.56 Nm) when actuated at 100 kPa, likely because the IPS increased the stiffness of the distal regions to match that of the center of the actuator. This is evidenced by the change in the deformed configuration of the two robots (Fig. 3.B). The unsupported robot yielded symmetrically in two distal regions consistent with [16] and no deformation was observed in the center. The supported robot yielded in three locations, a large deformation in the center of the actuator and two smaller distal deformations.

Torque measured at 0 kPa is used as a metric for how much the robot resists elbow extension. Resistance from the unsupported robot was negligible, whereas the supported robot started resisting extension at smaller angles due to the textile outer shell bunching between the two IPS.

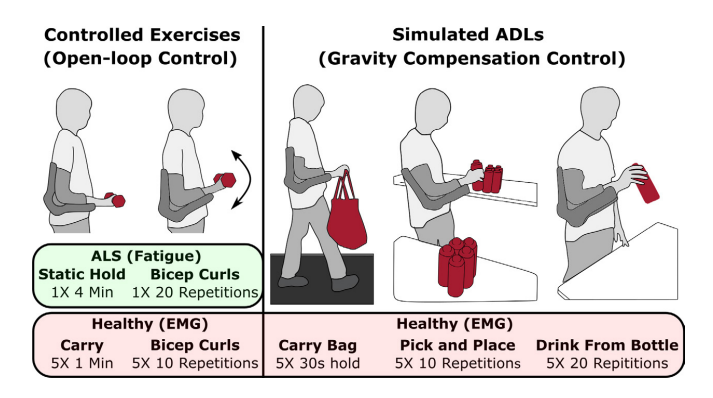


Fig. 4. Human subject evaluation protocol. ALS Controlled exercises (N=2), healthy controlled exercises (N=5), healthy simulated ADLs (N = 4, ADL protocol was skipped for one participant to keep overall study length within the 3-hour limit.)

E. Portability

The robot was integrated with a battery-powered PAU [8] to determine whether implementing the IPS increased portability. Portability is influenced by actuator torque, inflation time, and the number of actuations on a single charge [18]. Robots were evaluated by cyclically driving a mannequin arm loaded with 2.67 kg (6 Nm about the elbow) to 90° flexion. The unsupported robot required a $P_{flexion}$ of 100 kPa to reach 90° and 9.5 seconds to inflate and sustained 292 actuations. The long inflation time is a result of the depletion of the PAU's reservoir, requiring the PAU's compressor to partially fill the actuator at each cycle. The unsupported robot is not considered to be portable because inflation time is too slow to be practical for most applications. The supported robot operated at a lower pressure, lifting the arm with a $P_{flexion}$ of 80 kPa. It inflated in 1.7 seconds and sustained 496 actuations before running out of battery. The supported robot has similar system bandwidth to [8] and is considered to be portable.

III. HUMAN PARTICIPANT EXPERIMENTS

A. Evaluation in healthy individuals

A study was designed to evaluate the robot's ability to assist healthy subjects during both idealized and practical use cases (Fig. 4). 5 healthy participants (5 males; age: 25.0±3.4 years; mass: 71.6±9.8 kg; height: 1.79±0.07 m) were recruited. All participants gave written consent prior to participating and the protocols were approved by the Harvard Medical School Institutional Review Board under protocol IRB13-3418. Two surface electromyography (sEMG) sensors (Trigno Avanti, Delsys, USA), were placed on the Biceps Brachii and Triceps Brachii to measure muscle activity (data sampling at 2 kHz) [22]. The participants were then asked to perform a series of maximum voluntary contractions (MVCs) to define the baseline for maximum muscle activation used to normalize EMG results. Elbow ROM was measured with a goniometer (3 times with and without the robot). The participants were given some time to familiarize themselves with the robot and the exercise protocol was explained.

To evaluate ideal robot assistance participants performed static and dynamic exercises with the robot controlled using a pre-programmed pressure profile. In the dynamic exercise participants performed 5 sets of 10 bicep curls using a 4.5 kg dumbbell. $P_{flexion}$ alternated between 0 kPa and 100 kPa using a trapezoidal pressure profile (1 second linear ramp inflation from 0 kPa to 100 kPa, 1 second constant pressure hold at 100 kPa, and 1 second linear ramp deflation from 100 kPa to 0 kPa). A metronome was used to help the participants to keep motion consistent between assisted and unassisted trials. Truly static high-load holding tasks are less common than carrying tasks in everyday life. In the static exercise participants were asked to carry a 2.2 kg dumbbell at 90° for 1 minute while walking on a treadmill at 1 m/s. 5 sets were performed. $P_{flexion}$ was held constant at 100 kPa.

The practical assistance and controllability of the robot was evaluated using simulated ADLs. In all ADL trials, the robot was controlled using a gravity compensation controller based on our previous work for supporting the shoulder joint [8], [10]. Four inertial measurement units (IMUs) were placed on the torso, upper arms, and forearm to detect volitional movements of the limbs. The gravity compensation controller uses the pose of the limb to compute the desired pressure profile, which is controlled by a low-level pressure loop. Simulated ADLs are described in Fig. 4 and consist of 5 sets of carrying a 5 kg grocery bag for 30 seconds, 10 lateral pick and places of 1 kg bottle, and 20 simulated drinks from a 1 kg water bottle.

In all conditions, the robot was controlled by the PAU connected to wall air. The conditions with the device on and the device off were randomized for each participant. After initial fitting, IPS inflated to 200 kPa were used to tighten the sleeve during "on" conditions. The EMG data were first bandpass filtered (4th order, 10-400 Hz), then rectified before passing through a final low-pass filter (4th order, 10 Hz). Fig. 5 summarizes the results from the 5 conditions. Statistical analyses were conducted in MATLAB (MathWorks, USA). Results normalized against MVC are reported as the mean ± standard deviation. Shapiro-Wilk test was used to evaluate the normality of the data. Differences in muscle activity between 'on' and 'off' conditions were evaluated with paired t-test or Wilcoxon signed-rank test depending on normality of the data. Significant reductions in absolute % MVC in the biceps were found during the controlled static exercise (Fig. 5.A) as well as the simulated carry and drinking ADLs (Fig. 5.B). A non-statistically significant increase in triceps EMG was observed in one of the simulated ADLs (pick and place task). This is attributed to the gravity compensation controller because the wearer needs to act against the robot to initiate deflation to allow extension. The increase in triceps EMG was small, as seen in Fig. 5.B (0.9% of MVC), and is not expected to be biologically significant. The significance of change in absolute % MVC was negatively impacted by both small sample size and a large variability in participant's baseline strength as measured by unassisted % MVC.

Robot assistance is also commonly measured as the relative difference in EMG between the 'off' and 'on' conditions

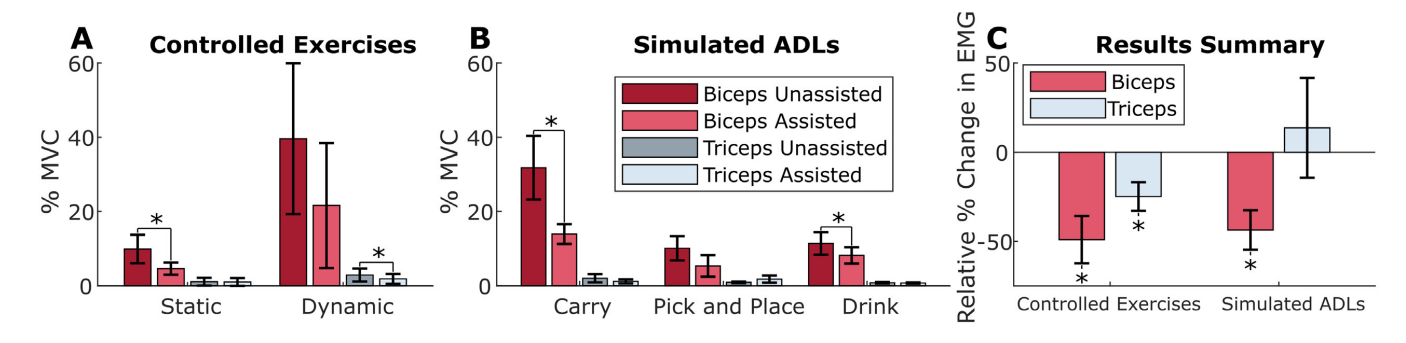


Fig. 5. A) % MVC required to complete controlled exercises for 'on' (assisted) and 'off' (unassisted) conditions. B) % MVC required to complete simulated ADLs. C) The average relative change in EMG between "on" and "off" conditions for each group of tasks. Robot-assisted resulted in a relative change in biceps EMG of $-49.1\pm13.3\%$ and $-43.6\pm11.1\%$ for the controlled exercises and simulated ADLs (negative relative % change in EMG is desirable). Error bar indicates standard deviation. *p < 0.05.

 $\label{thm:compact} \mbox{TABLE I} \\ \mbox{ROM results for healthy and ALS participants.}$

	Without Device	With Device On
Mean Range of Motion	146°±6°	134°±13°
(5 Healthy Participants)	$(0^{\circ}\pm3^{\circ} - 146^{\circ}\pm3^{\circ})$	(10°±6° - 144°±7°)
Range of Motion	137°±5°	121°±6°
(ALS Participant 1)	(12°±2° - 149°±3°)	$(10^{\circ}\pm2^{\circ} - 131^{\circ}\pm4^{\circ})$
Range of Motion	77°±6°	109°±10°
(ALS Participant 2)	(19°±5° - 96°±1°)	(15°±3° - 124°±7°)

[6], [8], [11], [12]. This metric is less sensitive to intersubject variability of participant strength. The relative reduction for each participant was averaged across the controlled exercises and simulated ADLs.

The significance of relative EMG reduction was measured using a paired t-test, as seen in Fig. 5.C. Significant reductions in relative biceps EMG were found in both the controlled exercises and simulated ADLs (-49.1±13.3% and -43.6±11.1% respectively), as well as in the triceps during controlled exercises (-24.9±8.0%).

Robot ROM is large enough to assist with approximately 90% of ADLs [3]. At the end of the protocol, no participants reported any discomfort related to the device; no bruising or skin irritation was observed after doffing the device.

B. Evaluation in individuals with ALS

A study was conducted to evaluate the performance of the robot in assisting individuals with ALS during the execution of controlled static and dynamic tasks (Fig. 4). ALS is a neurodegenerative disease that causes progressive loss of motor neurons in the brain and spinal cord resulting in loss of muscle control and disability [2].

Two participants diagnosed with ALS were recruited to participate in the study. Participant 1 (Female; age: 37 years; height: 1.65 m; mass: 113 kg; year diagnosed: 2018) was moderately impaired, being able to perform most upper-body ADLs with some difficulty. Participant 2 (Male; age: 74 years; height: 1.80 m; mass: 81 kg; year diagnosed: 2019) was severely impaired, being unable to perform most ADLs (Fig. 6). The study protocol was approved by the Harvard Medical School Institutional Review Board under protocol IRB13-3418. ROM of the participants was measured with a

goniometer (3 times with and without the robot). The participants familiarized themselves with the robot and the protocol was explained. $P_{flexion}$ was set based on each participant's comfort and perceived support (70 kPa for Participant 1 and 50 kPa for Participant 2). EMG was not collected due to discomfort caused by wearing the modules underneath the robot. Instead, fatigue and rate of perceived exertion (RPE) were used as an estimation of muscle activation.

The participants were asked to maintain a static hold (elbow flexed 90°) as long as they could. Participant 1 was loaded with 900 g weight strapped to the wrist (since the hand grip was affected). Participant 2 was not loaded due to his high level of impairment. $P_{flexion}$ was held constant at each participant's preferred pressure. The dynamic test consisted of performing 20 bicep curls. Participant 1 was loaded with 450 g around the wrist, and Participant 2 was not loaded. The actuation pressure alternated between 0 kPa and $P_{flexion}$ using a pressure sweep routine similar to the one described in Section III.A. A metronome was used to help the participants to keep motion consistent between assisted and unassisted trials. After each set of experiments, the participants were asked their RPE in both 'on' and 'off' conditions (on a scale from 1 to 10, 1 being extremely low effort and 10 being extremely high effort).

Both participants showed reduced fatigue when assisted by the device during the static hold. Participant 1's hold time increased from 32 seconds (unassisted) to 240 seconds (assisted) after which the experiment was stopped and her RPE decreased from 7 to 2. Participant 2's hold time increased from 21 seconds (unassisted) to 47 seconds (assisted) and his RPE decreased from 9 to 7. The robot reduced the effort to perform bicep curls in both participants. Participant 1 was able to complete the 20 repetitions in both conditions and her RPE decreased from 8 to 2 when assisted. Participant 2 was able to perform only 15 repetitions unassisted and was able to complete the 20 repetitions when assisted. His RPE decreased from 8 to 2. Due to participant 2's difficulty in controlling the shoulder rotation motion, the therapist supervising the study supported the participant's arm to keep the motion on the sagittal plane only. The support was provided in both device 'off' and 'on' test conditions.





Fig. 6. Elbow flexion device testing with Participant 1 (top) and Participant 2 (bottom).

The ROM of Participant 1 decreased by approximately 16° and for Participant 2 it increased by approximately 32°. Participant 1's ROM decrease is attributed to fitting as the sleeve was undersized. An increase in the ROM of Participant 2 was expected given the participant's high level of impairment and limited arm motion.

IV. CONCLUSIONS AND FUTURE DIRECTIONS

In this study, we proposed a soft inflatable robot that can assist the elbow flexion motion. The device was able to generate a level of torque throughout the elbow joint ROM that would be required during most ADLs. We demonstrated that partially filling the actuator volume with IPS increases actuator responsiveness and system bandwidth when driven by a PAU. To demonstrate the utility of the device to assist with human movement, we performed static and dynamic testing with both healthy and impaired populations. In healthy individuals, we found significant EMG reductions of the elbow flexors during controlled exercises (49.1±13.3%) indicating effective torque transfer to the wearer. We demonstrated the robot could be effectively controlled using an IMU-based gravity compensation controller resulting in 43.6±11.1% EMG reduction while performing simulated ADLs. For two individuals with ALS, we showed reduced fatigue, and reported reduced RPE. The average ROM when assisted by the device was 134°±13° for the healthy participants and 115°±8° for the ALS participants. While the device is effective at supporting elbow flexion, highly impaired participants may only receive limited assistance if additional joints are equally impaired. These results motivate us to extend our work, designing soft wearable robots with independently inflatable structures for assisting single and multiple joints.

REFERENCES

 "John hopkins medicine," https://www.hopkinsmedicine.org/health/ conditions-and-diseases/acute-spinal-cord-injury, access: Mar, 2023.

- [2] "The ALS association," https://www.als.org/, access: Feb, 2023.
- [3] A. Oosterwijk, M. Nieuwenhuis, C. v. d. Schans, and L. Mouton, "Shoulder and elbow range of motion for the performance of activities of daily living: A systematic review," *Physiotherapy Theory and Practice*, vol. 34, no. 7, pp. 505–528, 2018.
- [4] I. A. Murray and G. R. Johnson, "A study of the external forces and moments at the shoulder and elbow while performing every day tasks," *Clinical Biomechanics*, vol. 19, no. 6, pp. 586–594, 2004.
- [5] M. A. Gull, S. Bai, and T. Bak, "A Review on Design of Upper Limb Exoskeletons," *Robotics*, vol. 9, no. 1, p. 16, 2020.
- [6] M. Xiloyannis, D. Chiaradia, A. Frisoli, and L. Masia, "Physiological and kinematic effects of a soft exosuit on arm movements," *Journal* of NeuroEngineering and Rehabilitation, vol. 16, no. 1, p. 29, 2019.
- [7] C. Thalman and P. Artemiadis, "A review of soft wearable robots that provide active assistance: Trends, common actuation methods, fabrication, and applications," Wearable Technologies, vol. 1, 2020.
- [8] T. Proietti, C. O'Neill, L. Gerez, T. Cole, S. Mendelowitz, K. Nuckols, C. Hohimer, D. Lin, S. Paganoni, and C. Walsh, "Restoring arm function with a soft robotic wearable for individuals with amyotrophic lateral sclerosis," *Science Translational Medicine*, vol. 15, no. 681, p. eadd1504, 2023.
- [9] Y. M. Zhou, D. Wagner, K. Nuckols, R. Heimgartner, C. Correia, M. Clarke, D. Orzel, C. O'Neill, R. Solinsky, S. Paganoni, and C. J. Walsh, "Soft Robotic Glove with Integrated Sensing for Intuitive Grasping Assistance Post Spinal Cord Injury," 2019 International Conference on Robotics and Automation (ICRA), vol. 00, pp. 9059– 9065, 2019.
- [10] T. Proietti, C. ONeill, C. J. Hohimer, K. Nuckols, M. E. Clarke, Y. M. Zhou, D. J. Lin, and C. J. Walsh, "Sensing and Control of a Multi-Joint Soft Wearable Robot for Upper-Limb Assistance and Rehabilitation," *IEEE Robotics and Automation Letters*, vol. 6, pp. 2381–2388, 2020.
- [11] C. M. Thalman, Q. P. Lam, P. H. Nguyen, S. Sridar, and P. Polygerinos, "A Novel Soft Elbow Exosuit to Supplement Bicep Lifting Capacity," 2018 IEEE/RSJ International Conference on Intelligent Robots and Systems (IROS), vol. 00, pp. 6965–6971, 2018.
- [12] J. Nassour, G. Zhao, and M. Grimmer, "Soft pneumatic elbow exoskeleton reduces the muscle activity, metabolic cost and fatigue during holding and carrying of loads," *Scientific Reports*, vol. 11, no. 1, p. 12556, 2021.
- [13] T. H. Koh, N. Cheng, H. K. Yap, and C.-H. Yeow, "Design of a Soft Robotic Elbow Sleeve with Passive and Intent-Controlled Actuation," Frontiers in Neuroscience, vol. 11, p. 597, 2017.
- [14] J. Park, J. Choi, S. J. Kim, K.-H. Seo, and J. Kim, "Design of an Inflatable Wrinkle Actuator With Fast Inflation Deflation Responses for Wearable Suits," *IEEE Robotics and Automation Letters*, vol. 5, no. 3, pp. 3804–3810, 2019.
- [15] A. J. Veale, K. Staman, and H. v. d. Kooij, "Soft, Wearable, and Pleated Pneumatic Interference Actuator Provides Knee Extension Torque for Sit-to-Stand," Soft Robotics, vol. 8, no. 1, pp. 28–43, 2021.
- [16] I. M. Hasan, E. Q. Yumbla, and W. Zhang, "Development of a Soft Inflatable Exosuit for Knee Flexion Assistance," 2022 9th IEEE RAS/EMBS International Conference for Biomedical Robotics and Biomechatronics (BioRob), vol. 00, pp. 1–6, 2022.
- [17] S.-H. Park, J. Yi, D. Kim, Y. Lee, H. S. Koo, and Y.-L. Park, "A Lightweight, Soft Wearable Sleeve for Rehabilitation of Forearm Pronation and Supination," 2019 2nd IEEE International Conference on Soft Robotics (RoboSoft), vol. 00, pp. 636–641, 2019.
- [18] S. Joshi and J. Paik, "Pneumatic Supply System Parameter Optimization for Soft Actuators," Soft Robotics, vol. 8, pp. 152–163, 2021.
- [19] S. Sridar, S. Poddar, Y. Tong, P. Polygerinos, and W. Zhang, "Towards Untethered Soft Pneumatic Exosuits Using Low-Volume Inflatable Actuator Composites and a Portable Pneumatic Source," *IEEE Robotics* and Automation Letters, vol. 5, no. 3, pp. 4062–4069, 2019.
- [20] E. Siéfert, J. Bico, E. Reyssat, and B. Roman, "Geometry and mechanics of inextensible curvilinear balloons," *Journal of the Mechanics and Physics of Solids*, vol. 143, p. 104068, 10 2020.
- [21] C. M. McCann, C. J. Hohimer, C. T. O'Neill, H. T. Young, K. Bertoldi, C. J. Walsh, and C. M. McCann, "In-Situ Measurement of Multi-Axis Torques Applied by Wearable Soft Robots for Shoulder Assistance," *IEEE Transactions on Medical Robotics and Bionics*, vol. 5, no. 2, pp. 363–374, 5 2023.
- [22] "Recommendations for sensor locations on individual muscles [on-line]," seniam.org/sensor_location.htm, accessed: February, 2023.